Microporous MOFs

DOI: 10.1002/anie.201102329

A Microporous Copper Metal–Organic Framework with High H_2 and CO_2 Adsorption Capacity at Ambient Pressure**

*Daniel Lässig, Jörg Lincke, Jens Moellmer, Christian Reichenbach, Andreas Moeller, Roger Gläser, Grit Kalies, Katie A. Cychosz, Matthias Thommes, Reiner Staudt, and Harald Krautscheid**

Metal–organic frameworks (MOFs) as highly porous materials have gained increasing interest because of their distinct adsorption properties.[1–3] They exhibit a high potential for applications in gas separation and storage,[4] as sensors[5] as well as in heterogeneous catalysis.[6] In the last few years, the H_2 storage capacity of MOFs has been considerably increased. Mesoporous MOFs show high adsorption capacities for CH_4, CO_2, and H_2 at high pressures.[2,3,7–10] To increase the uptake of H_2 and CO_2 by physisorption at ambient pressure, adsorbents with small micropores as well as high specific surface areas and micropore volumes are required.[11,12] Such microporous materials seem to be more appropriate for gas-mixture separation by physisorption than mesoporous materials. For gas separation in MOFs the interactions between the fluid adsorptive and "open metal sites" (coordinatively unsaturated binding sites) or the ligands are regarded as important.[13] Industrial processes, such as natural-gas purification or biogas upgrading, can be improved with those materials during a vapor-pressure swing adsorption cycle (VPSA cycle) or a temperature swing adsorption cycle (TSA cycle).[14] The microporous MOF series CPO-27-M (M = Mg, Co, Ni, Zn), for example, shows very high CO_2 uptakes at low pressures (< 0.1 MPa).[15,16] Concerning H_2 adsorption, the microporous MOF PCN-12 offers with 3.05 wt% the highest uptake at ambient pressure and 77 K reported to date.[17]

Herein, we present a novel microporous copper-based MOF $^{3}_{\infty}$[Cu(Me-4py-trz-ia)] (**1**; Me-4py-trz-ia^{2-} = 5-(3-methyl-5-(pyridin-4-yl)-4*H*-1,2,4-triazol-4-yl)isophthalate) with extraordinarily high CO_2 and H_2 uptakes at ambient pressure, the H_2 uptake being similar to that in PCN-12. The ligand Me-4py-trz-ia^{2-} (Figure 1 a), which can be obtained from cheap starting materials by a three-step synthesis in good yield, combines carboxylate, triazole, and pyridine functions and is adopted from a recently presented series of linkers,[18] for which up to now only a few coordination polymers are known.[19–22]

Single crystals of **1** that are suitable for X-ray crystal structure analysis were prepared by diffusion of copper sulfate and H_2(Me-4py-trz-ia). Larger quantities of microcrystalline **1** are obtained not only by solvothermal synthesis, but also in multigram scale by simple reflux of the starting materials in water/acetonitrile (see Supporting Information).

According to the single crystal X-ray structure analysis, **1** crystallizes in the monoclinic space group $P2_1/c$ (no. 14) with four formula units per unit cell. The asymmetric unit contains one linker anion and two crystallographically independent Cu^{2+} ions residing on inversion centers. The copper ion Cu1 is coordinated in a square-planar fashion by two monodentate carboxylate and two pyridine functions in *trans* position leaving two accessible open metal sites per Cu1 atom (Figure 1 b), whereas the second copper ion Cu2 is coordinated by monodentate triazole and chelating carboxylate groups forming a distorted octahedron (Figure 1 c). For this reason, both copper ions represent planar fourfold nodal points and the ligands act as tetradentate linkers in a 3D network with **pts** topology[23] and a 3D pore system (Figure 1 d). With narrow channels of about 250 × 600 pm in crystallographic *c* direction connecting the micropores with a diameter of approximately 550 pm, the structure has a calculated porosity of about 55% according to PLATON.[24]

Powder X-ray diffraction (PXRD) studies on the as-synthesized microcrystalline sample **1a** confirm both, the agreement with the simulated powder pattern of **1** based on

---

[*] D. Lässig, J. Lincke, Prof. Dr. R. Gläser, Prof. Dr. H. Krautscheid
Universität Leipzig, Fak. für Chemie und Mineralogie
Johannisallee 29, 04103 Leipzig (Germany)
E-mail: krautscheid@rz.uni-leipzig.de

J. Moellmer, Dr. A. Moeller
Institut für Nichtklassische Chemie e.V.
Permoserstrasse 15, 04318 Leipzig (Germany)

C. Reichenbach, Dr. G. Kalies
Universität Leipzig, Fak. für Physik u. Geowissenschaften
Linnéstrasse 5, 04103 Leipzig (Germany)

Dr. K. A. Cychosz, Dr. M. Thommes
Quantachrome Instruments
1900 Corporate Drive, Boynton Beach, FL 33426 (USA)

Prof. Dr. R. Staudt
Hochschule Offenburg
Fak. für Maschinenbau und Verfahrenstechnik
Badstrasse 24, 77652 Offenburg (Germany)

[**] We gratefully acknowledge financial support by Deutsche Forschungsgemeinschaft (DFG SPP 1362-Poröse metallorganische Gerüstverbindungen, STA 428/17-1, KR 1675/7-1, GL 290/6-1; and KA 1560/3-2, 4-2), the University of Leipzig (PbF-1) and the graduate school BuildMoNa is gratefully acknowledged. D.L. thanks the Fonds der Chemischen Industrie for a fellowship, J.L. acknowledges the ESF fellowship. We thank F. Kettner for DTA/TG-MS analyses, Riaz Ahmad and Dr. Charlie Thibault (Quantachrome Instruments, US) for help with the N_2 (77 K), Ar (87 K) and H_2 (77, 87 and 97 K) sorption experiments on sample **1d**, and Dr. Angela Puls (Rubotherm GmbH, Bochum (Germany)) for measuring the N_2 (77 K) adsorption isotherms on sample **1a**.

Supporting information for this article is available on the WWW under http://dx.doi.org/10.1002/anie.201102329.

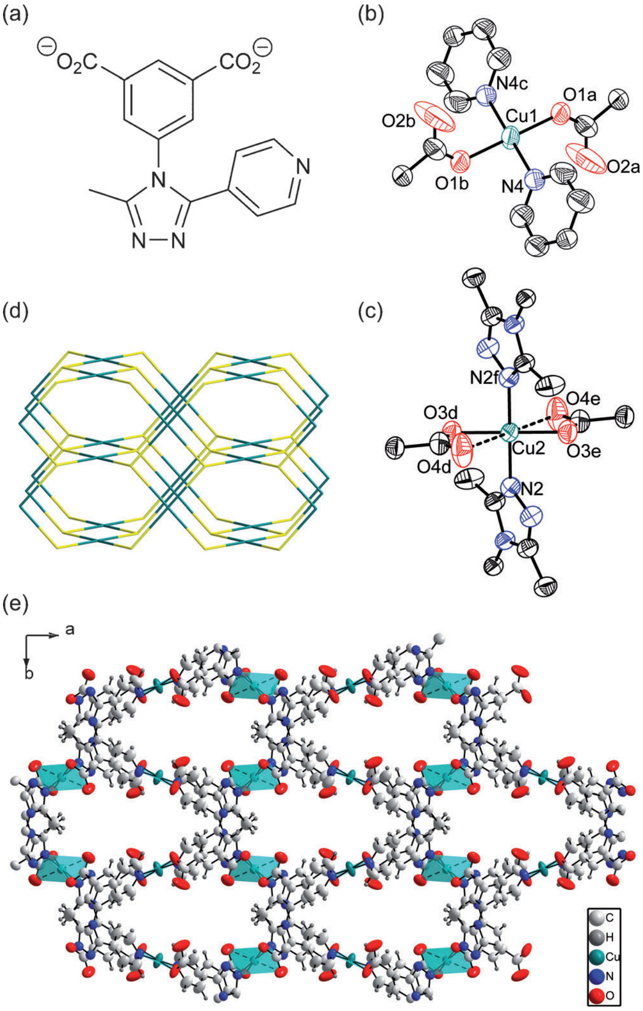

Figure 1. a) The ligand [Me-4py-trz-ia]$^{2-}$, b) and c) coordination spheres of both crystallographically independent Cu^{2+} ions in **1**, d) schematic drawing of the platinum sulfide topology (**pts**) of **1** (blue: square-planar Cu^{2+} nodal point; yellow: tetrahedral Me-4py-trz-ia^{2-} nodal point) and e) 3D crystal structure of **1** along [001]. Symmetry codes: a: 1−x, −0.5+y, 0.5−z; b: x, 0.5−y, 0.5+z; c: 1−x, −y, 1−z; d: x, 0.5−y, −0.5+z; e: −x, −0.5+y, 0.5−z; f: −x, −y, −z.

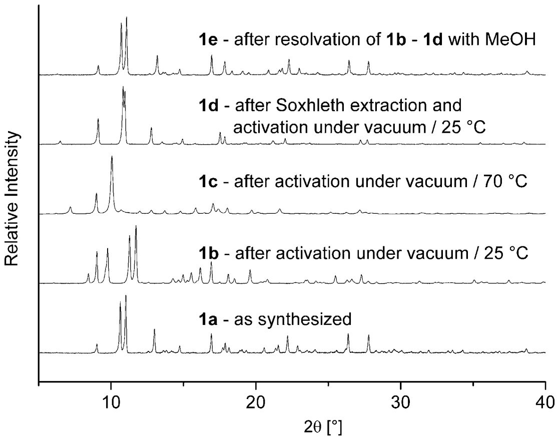

Figure 2. X-Ray powder patterns (Cu-K$_{\alpha 1}$) of microcrystalline samples of **1**: as-synthesized sample **1a**, samples **1b**–**1d** after postsynthetic treatment and sample **1e** after resolvation with methanol.

single crystal data and the phase purity of **1** obtained by different synthesis methods (Supporting Information, Figure S1).

Depending on the postsynthetic treatment, **1** represents a flexible network undergoing several phase transitions upon removal of and exposure to guest molecules. As shown in Figure 2, a treatment under vacuum at 25 °C (**1b**) and 70 °C (**1c**) leads to powder patterns different from that of the as-synthesized sample **1a**. A further phase transition is observed for a Soxhleth-extracted sample (MeOH) activated under vacuum at 25 °C (**1d**). However, if the dehydrated samples **1b**–**1d** are exposed to water or methanol, the powder pattern of **1a** is recovered (Figure 2). This indicates that the framework of **1** undergoes reversible crystal-to-crystal structural transformations.[25] The unit cell volumes determined from the powder patterns reveal shrinking upon activation (Table S1). In comparison to the as-synthesized **1a** phase, the activated phases **1b**, **1c**, and **1d** show unit cell volumes of 87 %, 70 %, and 72 %, respectively. This leads to the conclusion that **1d** has to expand during the adsorption process to allow the observed high uptakes reported herein.

According to temperature-dependent X-ray powder diffraction studies, the as-synthesized sample **1a** is thermally stable up to 140 °C. Soxhleth extraction with methanol significantly increases the stability up to 250 °C (**1d**), also shown by differential thermal analysis/thermogravimetry-mass spectrometry (DTA/TG-MS) studies. Although **1d** can be activated at 70 °C for adsorption measurements, an activation under vacuum at room temperature is sufficient to reach the maximum capacity. In case of **1a** the pores are partially blocked, resulting in only poor adsorption capacities (Figures S2 and S7). Hence for detailed adsorption studies, **1d** was used after activation at 25 °C for 48 h in vacuum.

N_2 (77.4 K) and Ar (87.3 K) isotherms are shown in Figure 3; Figure 3a shows the isotherms on a linear scale, and the type I N_2 isotherm (IUPAC classification[26]) indicates that as expected only micropores are present. An equivalent BET surface area of 1473 m^2 g^{-1} was obtained from the N_2 (77 K) isotherm (linear BET range p/p_0: 0.004 to 0.03). The total specific pore volume of 0.586 cm^3 g^{-1} determined from nitrogen adsorption (Table 1) is in perfect agreement with the specific pore volume of 0.59 cm^3 g^{-1} calculated from crystal structure data.[24] From the Ar and CO_2 adsorption on **1d**, a comparable total pore volume is determined (Table 1) indicating that the whole pore system of the MOF is open for these adsorptives at the respective conditions.

Figure 3b shows the N_2 and Ar adsorption data in a semilogarithmic plot, revealing details of the low-pressure regions of these isotherms, which are associated with the filling of micropores. The significant differences in the pore filling pressures between the Ar (87 K) and N_2 (77 K) sorption isotherms is interpreted as specific interactions between the quadrupolar N_2 molecules and the polar groups in the narrow pore channels of the MOF framework.[27] The relative pressure region where Ar (87 K) fills the pores of this copper MOF is for instance very similar to the relative

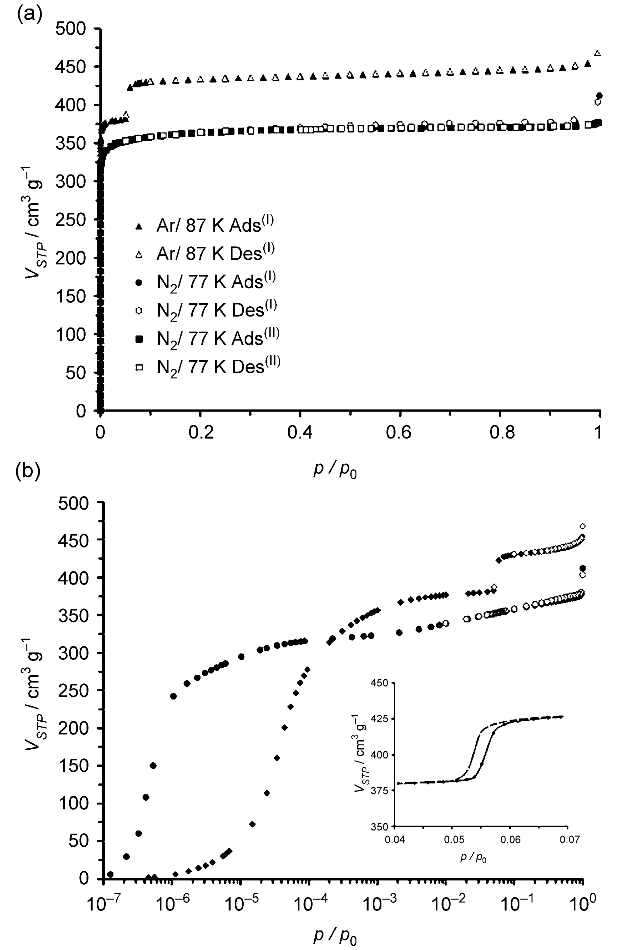

Figure 3. a) Nitrogen (77 K, squares and circles) and argon (87 K, triangles) adsorption isotherms on **1 d** (closed symbols = adsorption, open symbols = desorption; $^{(I)}$ measurements performed by Quantachrome Instruments Lab, US, $^{(II)}$ measurements performed by University of Leipzig, Germany). b) Semilogarithmic plot of nitrogen (circles) and argon (diamonds) adsorption isotherms (data from (a)) on **1 d** at 77 K and 87 K (closed symbols = adsorption, open symbols = desorption). Inset: hysteresis loop of argon adsorption isotherm at 87 K.

Table 1: BET specific surface area and pore volume of **1 d** calculated from adsorption isotherms at given relative pressures by means of the Gurvich rule.[30]

Adsorptive/Temperature	S_{BET} [m^{2}g^{-1}]	p/p_0	V_{Pore} [cm^{-3} g^{-1}]
N_2/77 K	1473	0.95	0.586[b]
Ar/87 K	1429[a]	0.04[a]/0.95[b]	0.485[a]/0.574[b]
CO_2/273 K	–	0.85	0.597[b]

[a] Before structural transformation. [b] After structural transformation.

pressure range where argon fills the narrow pores of a ZSM-5 zeolite.[28] Hence the effective degree of confinement for the adsorbate is comparable to the situation in ZSM-5, and accordingly the pore size distribution obtained by applying a NLDFT Ar (87.5 K) zeolite kernel based on a cylindrical pore model results in a narrow pore size distribution centered around 0.55 nm (Figure S4).

As already indicated, the Ar (87 K) isotherms reveal a sharp step at relative pressures of 0.05–0.06, which is accompanied by a narrow, but intrinsic hysteresis loop (see Figure 3 b and inset). The hysteretic adsorption behavior in that pressure range indicates a plausible structural transformation of the non-rigid material.[20,21,25,29] This transition appears also in the N_2 (77 K) isotherm, however it is reversible and smeared-out over a wider relative pressure range from 0.005–0.1.

CO_2 adsorption on **1d** was studied at 273 K, 298 K, and 323 K and used to calculate the isosteric heat of adsorption (Figures S8 and S9). All CO_2 isotherms are of type I according to the IUPAC classification.[26] The CO_2 uptake of **1d** was determined gravimetrically: 9.2 mmol g^{-1} (40.5 wt %) at 273 K/0.1 MPa and 6.1 mmol g^{-1} (26.8 wt %) at 298 K/0.1 MPa. Comparably high uptakes have been found so far only for very few microporous MOFs, for example, for the CPO-27-M series (M = Mg, Co, Ni, Zn).[15,31] For Ni- and Mg-containing CPO-27-MOFs isosteric heats of 38–42 kJ mol^{-1} were measured calorimetrically showing the high interaction energy between the quadrupolar CO_2 molecules and the open metal sites of the MOFs.[15] For the adsorption of CO_2 on **1d**, a constant isosteric heat of about 30 kJ mol^{-1} was calculated (see Supporting Information, Section 3.2.3), a similar value to that of HKUST-1 with 29.2 kJ mol^{-1}.[32]

To determine the hydrogen adsorption capacity, H_2 adsorption on **1d** (Figure 4) was measured at 77 K in the low pressure region (up to 0.1 MPa) using an automatic volumetric adsorption apparatus and in the high pressure region using a magnetic suspension balance. At 0.1 MPa/77 K, a remarkably high H_2 uptake of 15.2 mmol g^{-1} (3.07 wt %) of **1d** was determined, emphasizing the extraordinary adsorption potential of **1d** for H_2.

Additionally we obtained a maximum uptake of about 4.1 wt % at 3 MPa. This uptake does only roughly correlate to the established relation of 1 wt % H_2/500 m^2 g^{-1} BET surface

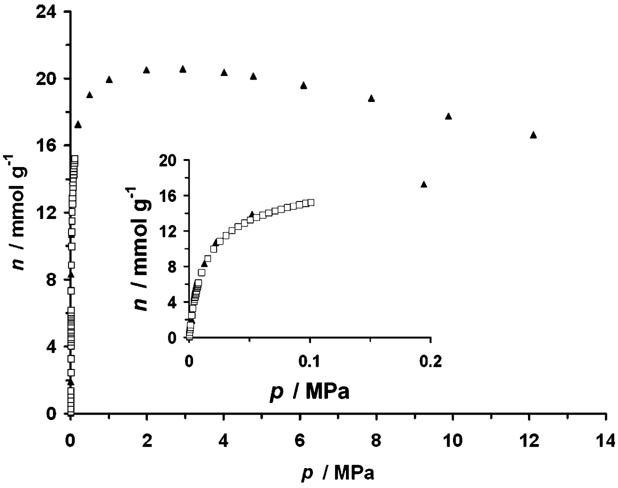

Figure 4. Hydrogen adsorption isotherm on **1 d** (triangles: excess adsorption, using magnetic suspension balance (INC Leipzig), squares: excess adsorption, using automatic volumetric adsorption apparatus (Quantachrome) at 77 K (inset: excess hydrogen adsorption up to 0.2 MPa).

area[10] and leads to the conclusion that the surface area determined from the N_2 adsorption isotherm (77 K) is underestimated, because the nitrogen molecules cannot occupy the inner surface on both sides of the micropore. Based on the H_2 isotherm, we therefore assume a potentially higher surface area.

The adsorption potential is confirmed by an isosteric heat of about 6.5 kJ mol^{-1} calculated from the adsorption isotherms at 77 K, 87 K, and 97 K (Figure S6). The constancy of the heat of adsorption is indicative of the homogeneity of the H_2 adsorption sites.[27] Therefore the strong interaction between the hydrogen molecules and the framework of **1d** is mainly attributed to the narrow micropores and the polar framework. To our knowledge, no MOF material has been reported so far with a higher H_2 uptake (15.2 mmol g^{-1}, 3.07 wt %) at ambient pressure at 77 K (Table 2).

Table 2: Hydrogen uptake of **1d** and selected MOF materials at 0.1 MPa and 77 K.

Material	wt %	Material	wt %
1d	3.07	In-soc-MOF[38]	2.60
PCN-12[17,33,34]	3.05	PCN-12-Si[12]	2.60
UTSA-20[35]	2.92	MOF-505[17,33]	2.59
SNU-5[33,34,36]	2.84	PCN-11[8,16,33]	2.55
NOTT-103[9]	2.63	CPO-27-Mg[37]	2.50
HKUST-1[17,33]	2.54–2.70	MOF-5[39]	1.32

For CO_2 on **1d**, we determined an uptake of 9.2 mmol g^{-1} (40.5 wt. %) at 273 K/0.1 MPa and 6.1 mmol g^{-1} (26.8 wt %) at 298 K/0.1 MPa, which is among the highest known for MOFs.

The adsorption isotherms for N_2 and H_2 were fully reproduced with several samples using two different adsorption devices. In this way, the persistent high quality of the synthesized material is impressively demonstrated. After exposure to ambient air, a reduced adsorption behavior was found, but it can be fully restored by Soxhleth extraction with MeOH and activation in vacuum.

In particular, the features outlined above make this new MOF material interesting for gas separation tasks. Preliminary results show that **1** is well suited for the separation of CO_2/CH_4 (separation factor >10) and CO_2/N_2 mixtures (separation factor >20).

In conclusion, the flexible microporous copper-based MOF material **1**, which is accessible in multigram scale amounts, has been characterized by means of X-ray crystal structure analysis, PXRD and adsorption measurements. Owing to the 3D narrow pore system **1** offers a high adsorption potential towards CO_2 and H_2 resulting in high gas uptakes at low pressures. From the universal sorption behavior towards different fluids as well as from a constant heat of adsorption for both CO_2 and H_2, we conclude that the good adsorption potential arises from the polar network and the narrow pore geometry itself rather than from specific interactions with open metal sites.

Experimental details associated with this article can be found in the Supporting Information version. CCDC 810290, 810291 contain the supplementary crystallographic data for this paper. These data can be obtained free of charge from The Cambridge Crystallographic Data Centre via www.ccdc.cam.ac.uk/data_request/cif.

Received: April 4, 2011
Revised: July 7, 2011

Keywords: adsorption · coordination polymers · copper · metal–organic frameworks · microporous materials

[1] a) M. Tonigold, Y. Lu, B. Bredenkötter, B. Rieger, S. Bahnmüller, J. Hitzbleck, G. Langstein, D. Volkmer, *Angew. Chem.* **2009**, *121*, 7682–7687; *Angew. Chem. Int. Ed.* **2009**, *48*, 7546–7550; b) M. Latroche, S. Surblé, C. Serre, C. Mellot- Draznieks, P. L. Llewellyn, J.-H. Lee, J.-S. Chang, S. H. Jhung, G. Férey, *Angew. Chem.* **2006**, *118*, 8407–8411; *Angew. Chem. Int. Ed.* **2006**, *45*, 8227–8231; c) R. Banerjee, A. Phan, B. Wang, C. Knobler, H. Furukawa, M. O'Keeffe, O. M. Yaghi, *Science* **2008**, *319*, 939–943.

[2] N. Klein, I. Senkovska, K. Gedrich, U. Stoeck, A. Henschel, U. Mueller, S. Kaskel, *Angew. Chem.* **2009**, *121*, 10139–10142; *Angew. Chem. Int. Ed.* **2009**, *48*, 9954–9957.

[3] H. Furukawa, N. Ko, Y. B. Go, N. Aratani, S. B. Choi, E. Choi, A. Ö. Yazaydin, R. Q. Snurr, M. O'Keeffe, J. Kim, O. M. Yaghi, *Science* **2010**, *329*, 424–428.

[4] a) D. M. D'Alessandro, B. Smit, J. R. Long, *Angew. Chem.* **2010**, *122*, 6194–6219; *Angew. Chem. Int. Ed.* **2010**, *49*, 6058–6082; b) M. Hartmann, S. Kunz, D. Himsl, O. Tangermann, S. Ernst, A. Wagener, *Langmuir* **2008**, *24*, 8634–8642; c) F. Debatin, A. Thomas, A. Kelling, N. Hedin, Z. Bacsik, I. Senkovska, S. Kaskel, M. Junginger, H. Müller, U. Schilde, C. Jäger, A. Friedrich, H.-J. Holdt, *Angew. Chem.* **2010**, *122*, 1280–1284; *Angew. Chem. Int. Ed.* **2010**, *49*, 1258–1262.

[5] a) C. A. Bauer, T. V. Timofeeva, T. B. Settersten, B. D. Patterson, V. H. Liu, B. A. Simmons, M. D. Allendorf, *J. Am. Chem. Soc.* **2007**, *129*, 7136–7144; b) B. V. Harbuzaru, A. Corma, F. Rey, P. Atienzar, J. L. Jordá, H. García, D. Ananias, L. D. Carlos, J. Rocha, *Angew. Chem.* **2008**, *120*, 1096–1099; *Angew. Chem. Int. Ed.* **2008**, *47*, 1080–1083.

[6] A. Corma, H. Garcia, F. X. Llabres i Xamena, *Chem. Rev.* **2010**, *110*, 4606–4655.

[7] A. G. Wong-Foy, O. Lebel, A. J. Matzger, *J. Am. Chem. Soc.* **2007**, *129*, 15740–15741.

[8] X.-S. Wang, S. Ma, K. Rauch, J. M. Simmons, D. Yuan, X. Wang, T. Yildirim, W. C. Cole, J. J. Lopez, A. de Meijere, H.-C. Zhou, *Chem. Mater.* **2008**, *20*, 3145–3152.

[9] X. Lin, I. Telepeni, A. J. Blake, A. Dailly, C. M. Brown, J. M. Simmons, M. Zoppi, G. S. Walker, K. M. Thomas, T. J. Mays, P. Hubberstey, N. R. Champness, M. Schröder, *J. Am. Chem. Soc.* **2009**, *131*, 2159–2171.

[10] a) M. Hirscher, *Angew. Chem.* **2011**, *123*, 605–606; *Angew. Chem. Int. Ed.* **2011**, *50*, 581–582; b) M. Hirscher, *Handbook of Hydrogen Storage*, Wiley-VCH, Weinheim, **2010**.

[11] A. Züttel, *Naturwissenschaften* **2004**, *91*, 157–172.

[12] S. E. Wenzel, M. Fischer, F. Hoffmann, M. Fröba, *Inorg. Chem.* **2009**, *48*, 6559–6565.

[13] G. J. Kubas, *Chem. Rev.* **2007**, *107*, 4152–4205.

[14] R. T. Yang, *Series on Chemical Engineering*, *Vol. I*, Imperial College Press, London, **1997**.

[15] P. D. C. Dietzel, V. Besikiotis, R. Blom, *J. Mater. Chem.* **2009**, *19*, 7362–7370.

[16] Z. Bao, L. Yu, Q. Ren, X. Lu, S. Deng, *J. Colloid Interface Sci.* **2011**, *353*, 549–556.

[17] X.-S. Wang, S. Ma, P. M. Forster, D. Yuan, J. Eckert, J. J. Lopez, B. J. Murphy, J. B. Parise, H.-C. Zhou, *Angew. Chem.* **2008**, *120*, 7373 – 7376; *Angew. Chem. Int. Ed.* **2008**, *47*, 7263 – 7266.

[18] D. Lässig, J. Lincke, H. Krautscheid, *Tetrahedron Lett.* **2010**, *51*, 653 – 656.

[19] J. Lincke, D. Lässig, H. Krautscheid, *Acta Crystallogr. Sect. C* **2009**, *65*, m488 – m490.

[20] J. Lincke, D. Lässig, J. Moellmer, C. Reichenbach, A. Puls, A. Moeller, R. Gläser, G. Kalies, R. Staudt, H. Krautscheid, *Microporous Mesoporous Mater.* **2011**, *142*, 62 – 69.

[21] C. Reichenbach, G. Kalies, J. Lincke, D. Lässig, H. Krautscheid, J. Moellmer, M. Thommes, *Microporous Mesoporous Mater.* **2011**, *142*, 592 – 600.

[22] D. Lässig, J. Lincke, J. Griebel, R. Kirmse, H. Krautscheid, *Inorg. Chem.* **2011**, *50*, 213 – 219.

[23] TOPOS, V. A. Blatov, A. P. Shevchenko, V. N. Serezhkin, *J. Appl. Crystallogr.* **2000**, *33*, 1193.

[24] PLATON, A. L. Spek, *J. Appl. Crystallogr.* **2003**, *36*, 7 – 13.

[25] S. Kitagawa, R. Kitaura, S. Noro, *Angew. Chem.* **2004**, *116*, 2388 – 2430; *Angew. Chem. Int. Ed. Engl.* **2004**, *43*, 2334 – 2375.

[26] K. S. W. Sing, D. H. Everett, R. A. W. Haul, L. Mouscou, J. Rouquerol, I. Siemieniewska, *Pure Appl. Chem.* **1985**, *57*, 603 – 619.

[27] J. Moellmer, E. B. Celer, R. Luebke, A. J. Cairns, R. Staudt, M. Eddaoudi, M. Thommes, *Microporous Mesoporous Mater.* **2010**, *129*, 345 – 353.

[28] M. Thommes in *Introduction to Zeolite Science and Practice*, 3rd rev. ed. (Eds.: J. Cejka, H. van Bekkum, A. Corma, F. Schüth), Elsevier, Amsterdam, **2007**, chap. 15, pp. 495 – 525.

[29] P. L. Llewellyn, S. Bourrelly, C. Serre, Y. Filinchuk, G. Férey, *Angew. Chem.* **2006**, *118*, 7915 – 7918; *Angew. Chem. Int. Ed.* **2006**, *45*, 7751 – 7754.

[30] L. Gurvich, *J. Phys. Chem. Soc. Russ.* **1915**, *47*, 805 – 827.

[31] S. R. Caskey, A. G. Wong-Foy, A. Matzger, *J. Am. Chem. Soc.* **2008**, *130*, 10870 – 10871.

[32] J. Moellmer, A. Moeller, F. Dreisbach, R. Gläser, R. Staudt, *Microporous Mesoporous Mater.* **2011**, *138*, 140 – 148.

[33] L. J. Murray, M. Dinča, J. R. Long, *Chem. Soc. Rev.* **2009**, *38*, 1294 – 1314.

[34] S. V. Kolotilov, V. V. Pavlishchuk, *Theor. Exp. Chem.* **2009**, *45*, 277 – 301.

[35] Z. Guo, H. Wu, G. Srinivas, Y. Zhou, S. Xiang, Z. Chen, Y. Yang, W. Zhou, M. O'Keeffe, B. Chen, *Angew. Chem.* **2011**, *123*, 3236 – 3239; *Angew. Chem. Int. Ed.* **2011**, *50*, 3178 – 3181.

[36] Y.-G. Lee, H. R. Moon, Y. E. Cheon, M. P. Suh, *Angew. Chem.* **2008**, *120*, 7855 – 7859; *Angew. Chem. Int. Ed.* **2008**, *47*, 7741 – 7745.

[37] P. D. C. Dietzel, P. A. Georgiev, J. Eckert, R. Blom, T. Strässle, T. Unruh, *Chem. Commun.* **2010**, *46*, 4962 – 4964.

[38] Y. Liu, J. F. Eubank, A. J. Cairns, J. Eckert, V. C. Kravtsov, R. Luebcke, M. Eddaoudi, *Angew. Chem.* **2007**, *119*, 3342 – 3347; *Angew. Chem. Int. Ed.* **2007**, *46*, 3278 – 3283.

[39] J. L. C. Rowsell, A. R. Millward, K. S. Park, O. M. Yaghi, *J. Am. Chem. Soc.* **2004**, *126*, 5666 – 5667.